Published in final edited form as:
Cancer Res. 2013 July 1; 73(13): 3852–3864. doi:10.1158/0008-5472.CAN-12-2353.

CRITICAL ROLE OF STAT3 IN IL-6-MEDIATED DRUG RESISTANCE IN HUMAN NEUROBLASTOMA

Tasnim Ara[1,5], **Rie Nakata**[1,5], **Michael A. Sheard**[1,5], **Hiroyuki Shimada**[2,5], **Ralf Buettner**[6], **Susan G. Groshen**[4], **Lingyun Ji**[4], **Hua Yu**[6], **Richard Jove**[6], **Robert C. Seeger**[1,5], and **Yves A. DeClerck**[1,3,5]

[1]Division of Hematology-Oncology, Department of Pediatrics, Keck School of Medicine of USC, Los Angeles

[2]Department of Pathology, Keck School of Medicine of USC, Los Angeles

[3]Department of Biochemistry & Molecular Biology, Keck School of Medicine of USC, Los Angeles

[4]Department of Preventive Medicine, Keck School of Medicine of USC, Los Angeles

[5]The Saban Research Institute of Children's Hospital Los Angeles, Los Angeles, California

[6]Department of Immunology and Cancer Biology, Beckman Research Institute, City of Hope, Duarte, California, USA

Abstract

Drug resistance is a major cause of treatment failure in cancer. Here we have evaluated the role of STAT3 in environment-mediated drug resistance (EMDR) in human neuroblastoma. We determined that STAT3 was not constitutively active in most neuroblastoma cell lines but was rapidly activated upon treatment with interleukin-6 (IL-6) alone and in combination with the soluble IL-6 receptor (sIL-6R). Treatment of neuroblastoma cells with IL-6 protected them from drug-induced apoptosis in a STAT3-dependent manner because the protective effect of IL-6 was abrogated in the presence of a STAT3 inhibitor and upon STAT3 knockdown. STAT3 was necessary for the upregulation of several survival factors such as survivin (BIRC5) and Bcl-xL (BCL2L1) when cells were exposed to IL-6. Importantly, IL-6-mediated STAT3 activation was enhanced by sIL-6R produced by human monocytes, pointing to an important function of monocytes in promoting IL-6-mediated EMDR. Our data also point to the presence of reciprocal activation of STAT3 between tumor cells and bone marrow stromal cells including not only monocytes but also Treg cells and non-myeloid stromal cells. Thus, the data identify an IL-6/sIL-6R/STAT3 interactive pathway between neuroblastoma cells and their microenvironment that contributes to drug resistance.

Keywords

Interleukin-6; STAT3; drug resistance; neuroblastoma; tumor microenvironment

Introduction

Over the last 10 years it has become increasingly appreciated that tumor cells that lack the intrinsic ability to initiate an angiogenic response, to resist the injury of therapies or to

Address correspondence to: Yves A. DeClerck, MD, 4650 Sunset Boulevard, MS#54, Los Angeles, CA 90027. Tel: 323-361-2150; Fax: 323-361-4902; declerck@usc.edu.

metastasize, can acquire such properties through the influence of the microenvironment (1). The acquisition of these properties occurs through complex interactions between tumor cells and a variety of stromal cells such as carcinoma-associated fibroblasts, endothelial cells, adipocytes, myofibroblasts, mesenchymal cells, and innate and adaptative immune cells (2–5). The identification of pathways involved in these interactions has therefore been the subject of intensive investigation over the recent years with the anticipation that these pathways will be novel targets for anti-cancer therapy (6). Among the characteristics that tumor cells acquire through their interaction with the microenvironment is drug resistance, a major cause of failure to eradicate cancer. The acquisition of drug resistance through interactions between tumor cells and their environment, known as “environment-mediated drug resistance” (EMDR) (7), is an important contributor to the emergence of minimal residual disease in cancer. EMDR occurs through complex adhesion-dependent and adhesion-independent interactions between tumor cells and the extracellular matrix (ECM) and stromal cells (8, 9). The bone marrow microenvironment plays a particularly important role in EMDR as it is an abundant source of ECM proteins, cytokines and growth factors produced by mesenchymal and hematopoietic stem cells and their progeny that promote homing and survival (10).

The bone marrow is also the most frequent site of metastasis in neuroblastoma, a tumor derived from the neural crest that is the second most common solid malignancy affecting children (11, 12). It is a source of multiple chemokines, cytokines and growth factors including interleukin-6 (IL-6). We have previously shown that in the case of neuroblastoma, IL-6 is not produced by tumor cells but by bone marrow-derived mesenchymal stem cells (BMMSC) and tumor-associated macrophages (TAM) (13–15). The paracrine production of IL-6 by BMMSC plays a dual role in neuroblastoma bone marrow and bone metastasis. It activates osteoclasts, promoting the formation of osteolytic lesions and stimulates the growth and survival of neuroblastoma cells (16). Among the signaling pathways activated by IL-6, is the Signal Transducer and Activator of Transcription (STAT)3 that plays a central role in the communication between tumor cells and immune cells (17). STAT3 was initially discovered as a transcription factor induced by interferon-γ (18). It is considered an oncogene as it is required for the oncogenic transformation activity of v-Src (19). It has multiple pro-tumorigenic functions including the promotion of tumor cell proliferation, survival, invasion, metastasis and angiogenesis (20–22). In addition, STAT3 is a major contributor to inflammation (23) and has been shown to promote the acquisition of chemo- and radio-resistance (24, 25). In most cancers STAT3 is constitutively active, but its activation can also occur through the influences of the microenvironment and in particular IL-6 (26). IL-6 binds to an heterodimeric receptor made of two subunits, the gp80 α subunit (IL-6R) that is the ligand binding unit and the gp130 β subunit that is the signal transducing unit which via phosphorylation of Janus Kinases (JAK), activates STAT3 (27/xref>). The gp80 unit is also present in a soluble form (sIL-6R) that has an agonistic effect through its trans signaling function (28). Here we have explored the role of STAT3 activation by IL-6 and sIL-6R in EMDR in human neuroblastoma.

Materials and Methods

Cell culture

Human neuroblastoma cell lines were cultured as previously reported (16). The cells were authenticated by genotype analysis using AmpFISTR Identifier PCR kit and GeneMapper *ID* v. 3.2 (Applied Biosystems). Human BMMSC were purchased from AllCells LLC. Monocytes of normal healthy donors were obtained from peripheral blood and separated by Ficoll density gradient centrifugation using a human monocyte isolation kit (Miltenyi Biotech).

Reagents

Rabbit polyclonal antibodies against pY^{705} STAT3, STAT3, survivin, Bcl-xL XIAP, Bcl-2, Mcl-1, uncleaved and cleaved caspase 3 and 9, and cytochrome C and Alexa Fluor 488-conjugated antibodies against survivin and Bcl-xL were purchased from Cell Signaling Technology, Inc. A rabbit polyclonal antibody against actin and a mouse monoclonal antibody (mAb) against β-actin were purchased from Sigma-Aldrich. A mouse polyclonal antibody against STAT3 was purchased from Cell Signaling Technology, Inc. The following secondary antibodies were used for Western blots, immunocytofluorescence and immunohistochemistry: biotinylated anti rabbit IgG (H+L) (Vector Labs), donkey anti rabbit IRDye 800CW, donkey anti mouse IRDye 680 (LI-COR Biosciences), goat horseradish peroxidase conjugates anti rabbit Streptavidin Dylight 488 (Jackson Immunoresearch), goat anti mouse Alexa Fluor 555 (Invitrogen) and donkey anti rabbit IgG (Thermo Scientific). Antibodies against the following markers were from BD Biosciences (San Diego, CA): CD14-V450, phospho-Stat3 (pY705) -PE, CD4-APC-H7, CD25-PE-Cy7, FoxP3-PerCP-Cy5.5, GD2-APC. Anti-CD3-AlexaFluor488 was from BioLegend (San Diego, CA). Anti-CD163-AlexaFluor700 was from R&D Systems (Minneapolis, MN). Anti-CD45-Krome Orange was from Life Technologies (Grand Island, NY). Human FcR blocking agent was from Miltenyi Biotec (Cambridge, MA). BD Fix I Buffer and BD Perm III Buffer were from BD Biosciences. Etoposide (Ben Venue Laboratories, Inc.) and melphalan (Sigma-Aldrich) were dissolved in acidified-ethanol at a stock concentration of 64 μg/mL. The STAT3 inhibitor stattic (29) was purchased from Calbiochem and solubilized in dimethylsulfoxide (DMSO) at a stock concentration of 60 mmol/L. Recombinant human IL-6 and sIL-6R were purchased from R&D Systems. A humanized mouse monoclonal function blocking antibody against IL-6R (tocilizumab) (30) was purchased from Genentech, Inc.

Western blot

Western blots were performed as previously described (16). Cells were lysed in RIPA buffer supplemented with 1 tablet of complete mini-EDTA protease inhibitor cocktail (Roche Diagnostics) or halt protease and phosphatase inhibitor cocktail (Thermo Scientific). The detection of immune complexes and their quantification was performed using either the Odyssey Infrared Imaging Systems (LI-COR Biosciences) or chemiluminescence with an HRP antibody detection kit (Denville) and the NIH ImageJ software for analysis.

Cell viability assay

Cell viability in the presence of cytotoxic drugs was determined by fluorescence-based cytotoxicity assay using digital imaging microscopy (DIMSCAN) (31).

Flow cytometry

For JC-1 stain, cultured cells were detached in cell dissociation buffer (Invitrogen) and stained for 30 minutes in the presence of JC-1 dye (10 mg/mL; MitoProbe JC-1 assay kit from Invitrogen) before being analyzed by flow cytometry. For annexin V stain, cultured cells were resuspended in 1 × annexin V binding buffer. Annexin V and propidium iodide (PI) staining were performed using an annexin V-FITC apoptosis detection kit II according to the manufacturer's instructions (BD Pharmingen).

ELISA assay

The levels of human IL-6 and sIL-6R in serum free conditioned medium of cultured cells were determined by ELISA using the Quantikine Immunoassay kit or DuoSet ELISA development kit from R&D Systems.

siRNA based gene knockdown

Downregulation of the expression of STAT3 was done using the Signal Silence STAT3 siRNA kit (Cell Signaling Technology, Inc.). Cells plated in 6 well plates (2.5×10^5 cells) were transfected with scrambled siRNA or STAT3 siRNA and a fluorescein conjugated siRNA (to verify transfection efficiency) using the Lipofectamine RNAi MAX reagent (Invitrogen). The downregulation of the protein (STAT3) was verified by Western blot analysis on cell lysates obtained 72 hours after transfection. The following siRNA sequences were used from SignalSilence: STAT3 siRNAII, cat. no. 6582 and STAT3 siRNA I, cat. no. 6580.

Immunohistochemistry and immunofluorescence

Paraffin-embedded sections (4 μm) of bone marrow biopsies were obtained through the Children's Oncology Group (COG) Biorepository by H.S. These samples were acquired after informed consent was obtained and upon approval of CHLA's Institutional Review Board. Antigen unmasking was performed by proteinase K treatment (20 μg/mL for 10 minutes at 25°C). The slides were incubated overnight at 4°C in the presence of the following primary antibodies: a rabbit anti human pY705 STAT3, survivin, or Bcl-xL, a mouse anti CD68 or a rabbit anti-tyrosine hydroxylase (TH) mAb (dilutions 1:100). After washing 3× with 0.1% Triton-X 100 in phosphate buffer saline, the slides were incubated in the presence of one of the following secondary antibodies: an Alexa-Fluor 488 conjugated goat anti mouse IgG, or anti mouse IgG antibody (dilution 1:50) for 1 hour at room temperature. For immunofluorescence, slides were mounted in DAPI containing Vectashield medium. For dual immunohistochemistry, the Bond Polymer Refine Detection (Leica Biosystems Newcastle Ltd, Newcastle upon Tyne, UK) was used. Slides were heated at pH6 for 20 minutes before being processed. The biotin-free polymeric horse radish peroxidase linker (DS 9800) was used for the detection of pSTAT3 and the biotin-free polymeric alkaline phosphatase linker (DS 9390) was used for the detection of Protein Gene Product (PGP) 9.5 and CD45. As primary antibodies we used a mouse anti-human PGP 9.5 from Leica (PA0286) undiluted, a mouse anti-CD45 mAb from Abcam (ab8216) at a 1:25 dilution and a rabbit anti pSTAT3 (Tyr705) polyclonal antibody from Cell Signaling (9131) at a 1:25 dilution. Primary and secondary antibodies were incubated for 30 minutes.

Immunocytofluorescence

Cells were cultured in Lab-Tek II 8 chamber slides for 48 hours (2×10^4 and 10×10^4 cells/well). Cells were then washed, treated with IL-6 and sIl-6R for 30 minutes and then fixed with 4% formaldehyde in PBS for 10 minutes and permeabilized with 0.1% Triton-X100 in 15% FBS in PBS for 5 minutes, before being incubated in the presence of an anti-human pSTAT3 or STAT3 antibody overnight at 4°C.

Statistical analysis

For the analyses of cell viability, the luciferase or fluorescence activity readings were assumed to have a lognormal distribution and were transformed to the log 10 scale before analyses were conducted. Analysis of Variance (ANOVA) was used to examine the differences in mean cell viability among groups and the Student (two tailed) test was used to compare two groups in the apoptotic assays. All p values reported were two-sided. A p value of less than 0.05 was considered significant. Data were analyzed with software STATA version 11.2 (StataCorp LP, College Station, TX).

Results

IL-6 and sIL-6R activate STAT3 in neuroblastoma cells

We had previously reported that with a few exceptions most human neuroblastoma cells do not produce significant amounts of IL-6 and do not secrete sIL-6R, but express the two IL-6R subunits (16). To determine the status of STAT3 activation in neuroblastoma, we initially examined 8 human tumor cell lines for the expression of STAT3 and phospho Y^{705} STAT3 (pSTAT3) by Western blot under baseline conditions and upon treatment with IL-6, sIL-6R and their combination. This analysis revealed a low amount of pSTAT3 in most untreated cells (except in SK-N-SH and CHLA-90 cells), indicating a general absence of constitutive activation of STAT3 in neuroblastoma (Fig. 1A). However, when cells were treated with IL-6 alone and in particular in combination with sIL-6R, we observed a significant increase in pSTAT3 after 30 minutes in all cell lines. Activation of STAT3 in CHLA-255 and CHLA-90 cells was confirmed by immunocytofluorescence (Fig. 1B). This analysis revealed the presence of cytoplasmic STAT3 in both cell lines. In CHLA-255 cells, pSTAT3 was not detected in the absence of IL-6 but became detectable in the nucleus upon treatment with IL-6 alone or in combination with sIL-6R. In contrast, nuclear pSTAT3 was detected in CHLA-90 cells with or without treatment with IL-6 and sIL-6R. To confirm the role of IL-6 in STAT3 activation, we demonstrated that incubation of CHLA-255 cells with a monoclonal antibody against human IL-6R (tocilizumab) prior to treatment with IL-6 and IL-6 plus sIL-6R suppressed STAT3 phosphorylation (Supplemental Fig. 1A) and the binding of STAT3 to DNA as determined by electrophoretic mobility shift assay (EMSA) (Supplemental Fig. 1B). We also demonstrated that CHLA-255 cells transiently transfected with a STAT3 responsive promoter construct driving the firefly luciferase reporter gene (STAT3Fluc) and a renilla luciferase vector had a 4 fold increase in firefly/renilla luciferase activity when treated with IL-6 plus sIL-6R, and that this increase in activity was suppressed in the presence of tocilizumab (Supplemental Fig. 1C). Thus, altogether the data demonstrated that IL-6 is an effective and specific activator of STAT3 in human neuroblastoma, in particular in the presence of sIL-6R.

IL-6 and sIL-6R protect neuroblastoma cells from drug-induced apoptosis

To demonstrate the role of IL-6 in chemoresistance, we selected two drug sensitive neuroblastoma cell lines (CHLA-255 and SK-N-SH) and tested the effect of IL-6 and sIL-6R on their survival in the presence of etoposide and melphalan (32–33). This analysis revealed a dose-dependent decrease in the survival fraction in both cell lines upon exposure to etoposide or melphalan for 24 hours (Fig. 2A to D). However, when cells were pre-treated with IL-6 (alone and with sIL-6R) and then exposed to the drug, we observed a significant increase in the survival fraction when compared with the drug alone. As anticipated, the addition of sIL-6R alone in the absence of IL-6 failed to protect neuroblastoma cells from etoposide-induced apoptosis (Supplemental Fig. 3A). We next examined the effect of IL-6 and sIL-6R pre-treatment on mitochondrial membrane depolarization and caspase 3 and 9 activation in cells treated with etoposide or melphalan (Fig. 3). The data demonstrated that pre-treatment of CHLA-255 cells with IL-6 alone or with sIL-6R resulted in less mitochondrial membrane depolarization (Fig. 3A and B). IL-6 also inhibited the cytoplasmic release of cytochrome C upon treatment with etoposide (Fig. 3C). Consistently, pre-treatment of CHLA-255 cells with IL-6 inhibited the cleavage of caspase 3 and caspase 9 in the presence of increased concentrations of etoposide or melphalan (Fig. 3D and E). Altogether the data thus indicated that IL-6 had a protective effect on drug-induced intrinsic apoptosis.

STAT3 is necessary for IL-6-mediated drug resistance

We next asked the question whether STAT3 activation was necessary for the protective effect of IL-6 on drug-induced apoptosis. We first used stattic, a small molecule inhibitor of STAT3 activation (29) and demonstrated that treatment of CHLA-255 cells with stattic (0.5 to 20 μM) prevented STAT3 activation by IL-6 plus sIL-6R (Fig. 4A). We then examined the effect of stattic (at 2.5 μM, to maintain 80% cell viability) on apoptosis induced by etoposide in CHLA-255 cells pre-treated with IL-6 and sIL-6R. The data indicated that stattic restored etoposide-induced apoptosis in the presence of IL-6 and IL-6 plus sIL-6R to levels observed in the absence of IL-6 and stattic (Fig. 4B).

The necessary role of STAT3 in IL-6-mediated drug resistance was confirmed by examining the effect of siRNA-mediated STAT3 knockdown (KD) on neuroblastoma cell sensitivity to etoposide in the presence of IL-6 and sIL-6R. The data indicated that transfection of CHLA-255 cells with a combination of two siRNA sequences resulted in an 80% STAT3 KD and a complete suppression of STAT3 activation upon treatment with IL-6 alone or with sIL-6R when compared with a scramble siRNA sequence (Fig. 4C). STAT3 KD in CHLA-255 cells restored their sensitivity to etoposide in the presence of IL-6 and sIL-6R to levels close to the level of apoptosis observed in the absence of IL-6 (Fig. 4D). The KD of STAT3 in SK-N-SH cells had a similar effect on the sensitivity of these cells to etoposide in the presence of IL-6 and sIL-6R (Supplemental Fig. 2A and B). The data thus demonstrated that the protective effect of IL-6 on drug-induced apoptosis in neuroblastoma was STAT3 activation-dependent.

Upregulation of survival proteins by IL-6 is STAT3-dependent

We investigated the effect of IL-6 on the expression of survival proteins in CHLA-255 cells. The data indicated an increase in the expression of survivin Mcl-1, XIAP-1 and Bcl-xL (Fig. 5A). An upregulation of survivin and Bcl-xL (to a lesser extend) was also observed in SK-N-SH cells treated with IL-6 (Supplemental Fig. 2C). We then demonstrated that the upregulation of some of these survival proteins was STAT3-dependent by showing that stattic inhibited the nuclear expression of survivin in CHLA-255 cells treated with IL-6 and IL-6 + sIL-6R (Fig. 5B) and by documenting a marked decrease in survivin expression and an absence of Bcl-xL expression upon STAT3 KD in cells treated with IL-6 and IL-6 plus sIL-6R (Fig.5C). The data suggested that STAT3 –dependent up regulation of survival factors like survivin and Bcl-xL was a mechanism by which IL-6 protected neuroblastoma cells from apoptosis.

BMMSC and monocytes cooperate to sensitize neuroblastoma cells to IL-6-mediated STAT3 activation

Our *in vitro* data consistently demonstrated that IL-6 was more active on neuroblastoma cells in the presence of sIL-6R. This suggested that sIL-6R sensitized neuroblastoma cells to STAT3 activation by IL-6. To test this hypothesis, we examined whether the addition of sIL-6R at a concentration of 25 ng/mL, which is within the range of the levels detected in the blood of patients with neuroblastoma (10–90 ng/mL; Ref. 34, 35), would result in STAT3 activation in the presence of concentrations of IL-6 in the (0.1 to 10) ng/mL range. These experiments demonstrated that when IL-6 was used alone, a concentration of 10 ng/mL was necessary to activate STAT3 whereas when used in combination with sIL-6R (25 ng/mL), a concentration of 0.1 ng/mL of IL-6 was sufficient for STAT3 activation (Fig. 6A). We then tested whether activation of STAT3 in the presence of 10 ng/mL of IL-6 could be potentiated by lower concentrations of sIL-6R. The data (Figure 6B) demonstrated an increase in pSTAT3 activation in the presence of 10 ng/mL of sIL-6R and above but not at lower concentrations (0.1 and 1.0 ng/mL). These sIL-6R concentrations are found the blood of cancer patients (35). Because neuroblastoma cells do not produce sIL-6R and are thus

dependent of a paracrine source (16), we examined whether it was produced by normal cells in the tumor microenvironment. We first tested BMMSC which we had previously shown to be a source of IL-6 (13). The data demonstrated an anticipated increase in the production of IL-6 (to 1600 pg/mL) when BMMSC were co-cultured with CHLA-255 cells and low amount of sIL-6R (Mean 32.5 ± 14.8 pg/mL; Fig. 6C, upper panel). We then tested human monocytes which we had also shown to be a source of IL-6 (14). This experiment revealed that monocytes produced IL-6 and sIL-6R in culture and that their production was significantly increased in the presence of CHLA-255 cells. The amount of sIL-6R produced (Mean 149.5 ± 8.6 pg/mL) in the presence of CHLA-255 was 5 fold higher than BMMSC in similar conditions (Fig. 6C, lower panel). Although this concentration is lower than the concentration required to enhance STAT3 activation in vitro (Fig. 6B), we demonstrated that when human monocytes were co-cultured with CHLA-255 cells, STAT3 became activated in the tumor cells even in the presence of low amounts of IL-6 (20 pg/mL) and that activation was in part IL-6R-dependent since it was partially inhibited in the presence of tocilizumab (Fig. 6D). The data thus point to the important contributory function of monocytes to STAT3 activation that is in part mediated by IL-6 and sIL-6R but could involve other activators. We also asked whether STAT3 would be activated in monocytes when in the presence of neuroblastoma cells. In this experiment CHLA-255 cells and human monocytes were cultured alone or in contact for 24 hours and the mixture of cells was analyzed for the presence of nuclear pSTAT3 and cell surface CD 14 (monocytes) and CD 56 (neuroblastoma). The data (Fig. 6E and supplemental Fig. 3B) indicated an absence of pSTAT3 in cells cultured alone but a significant increase in pSTAT3 in both tumor cells and monocytes after 24 hours of co-culture, indicating the presence of a reciprocal STAT3 activation loop between neuroblastoma cells and monocytes.

STAT3 is activated in the bone marrow microenvironment in patients with metastatic neuroblastoma

To provide evidence for a role of STAT3 in patients with metastatic neuroblastoma, we examined STAT3 activation in a series of 10 bone marrow biopsies obtained from children with neuroblastoma. Five specimens were classified as positive for tumor involvement in the marrow (as assessed by the presence of TH positive cells by immunohistochemistry ; Ref 36) and 5 were classified as negative for tumor cells. An analysis of the presence of nuclear pSTAT3 positive cells in these samples revealed a higher percentage (22.3% ± 6.06) of nuclear pSTAT3 in samples with tumor cells and a lower percentage (7.9% ± 1.8 ; p=0.002) in samples negative for tumor cells (Fig. 7A). There was also a higher number of survivin positive cells in samples infiltrated with tumor cells than in samples without tumor cells (122 ± 69 versus 10 ± 14 respectively) and a higher level of Bcl-xL expression (Supplemental Fig. 3C). Because our in vitro co-culture experiments on tumor cells and monocytes indicated a reciprocal activation of pSTAT3 (Fig. 6D and E), we then asked the question whether STAT3 was activated in tumor cells and stromal cells in the bone marrow of patients with neuroblastoma. An analysis of pSTAT3 and CD45 by double immunohistochemistry on a bone marrow biopsy sample containing >90% tumor cells (Fig. 7B) indicated that 93% of PGP9.5 positive tumor cells were also pSTAT3 positive and that 42% of CD45 positive myeloid cells were also positive for pSTAT3. By double immunofluorescence with an anti-CD68 antibody, we then demonstrated the presence of nuclear pSTAT3 in CD68 positive monocytes/macrophages. The data are consistent with our in vitro co-culture experiment (Fig. 6E) and indicate that STAT3 in the bone marrow microenvironment is not only activated in tumor cells but also in myeloid cells including monocytes/macrophages (Fig. 7C). To better define sub-populations of these pSTAT3 positive myeloid cells, we examined by flow cytometry an additional 8 fresh bone marrow samples from neuroblastoma patient for the presence of nuclear pSTAT3 (Supplemental Fig. 4A). Using a combination of 6 surface markers (CD3, CD4, CD14, CD25, CD 45 and GD2

and one nuclear marker FoxP3), we identified 6 populations of cells with $CD45^{-}/GD2^{-}$ (non-myeloid), $CD45^{+/}CD14^{-}$ (myeloid non-monocytic) and $CD45^{+/}CD14^{+}$ (monocytic) being the most (>10% of total mononuclear cells) abundant (Supplemental Fig.4B). An analysis of pSTAT3 in these different populations, indicated a greater than 10% positive cells in 4 subpopulations, $CD45^{-}/GD2^{-}$ non-myeloid, non-tumor cells, $CD45^{-}/GD2+$ tumor cells, $CD45^{+}/CD14^{+}$ monocytes and $CD45^{+}/CD3^{+}/CD4^{+}/CD25^{+}/FoxP3^{+}$ Treg cells indicating that in addition to monocytes, Treg and non-myeloid cells could be part of the reciprocal loop of STAT3 activation between tumor cells and bone marrow-derived cells. Thus our data identify an IL-6/sIL-6R/STAT3 interactive pathway between neuroblastoma cells and the tumor microenvironment that contributes to drug resistance and in which STAT3 has a necessary function.

Discussion

Overexpression of IL-6 by BMMSC has a dual pro-tumorigenic function on neuroblastoma cells by promoting osteoclast activation (13) and tumor cell proliferation and survival (16). Here we demonstrate the presence of an IL-6/sIL-6R/STAT3 paracrine pathway of interaction between tumor cells and the microenvironment that provides tumor cells with the ability to counteract the apoptotic effect of cytotoxic agents. Constitutive activation of STAT3 by oncogenes such as Src, Fes, Sis, PyMT, Ros or Eyk has been reported (37) but not by MYC-N, which is often amplified in neuroblastoma (38). Among the 8 cell lines examined one, SK-N-BE(2), exhibited amplification of the MYC-N oncogene and in this cell line--as in most other cell lines without MYC-N amplification--STAT3 was not constitutively active. Our data indicate that in contrast to many other types of cancer, STAT3 activation is rarely constitutive in neuroblastoma but seems dependent on the tumor microenvironment. Although our data specifically point to a role for IL-6 as activator of STAT3, they do not rule out the possibility that other cytokines and growth factors could also contribute.

Our data identify a central function for the IL-6/sIL-6R/STAT3 pathway in conferring drug resistance to neuroblastoma cells. This effect involves the upregulation of several anti-apoptotic proteins in particular survivin, Bcl-xL, Mcl-1 and XIAP that are known transcriptional targets of STAT3 (25, 39, 40). The observation that survivin is downstream of STAT3 signaling is relevant since high levels of survivin in neuroblastoma have also been associated with poorer clinical outcome (41). It has been previously reported that IL-6 - mediated STAT3 activation plays a role in EMDR in myeloma (42), however the mechanisms involved seem different between the two types of cancer. In myeloma, activation of STAT3 by IL-6 is primarily mediated by β1 integrin-dependent adhesion of myeloma cells to bone marrow stromal cells (8). In contrast, in neuroblastoma the expression of IL-6 in the bone marrow stroma is primarily regulated by soluble factors produced by tumor cells including prostaglandin E2 (16) and galectin-3 binding protein (43) among others.

Our data provide a new insight into the contributory role of monocytes to STAT3 activation by demonstrating that monocytes produce sIL-6R and that sIL-6R enhances the sensitivity of neuroblastoma cells to IL-6-mediated STAT3 activation. The importance of sIL-6R in IL-6/gp130 signaling in autoimmunity, inflammation and cancer has been recently emphasized (44). Elevated levels of sIL-6R have been reported in the blood of patients with cancer including neuroblastoma and myeloma, and are typically a marker of unfavorable clinical outcome (34, 35, 45). These blood levels (ng/mL) are higher by 100 fold than the in vitro concentration of sIL-6R observed in co-cultures of neuroblastoma cells and human monocytes. Although the reason for this discrepancy is not entirely clear, our data demonstrate a strong activation of STAT3 in co-cultures of neuroblastoma cells and

monocytes that is in part suppressed by a blocking antibody against IL-6R supporting a potentiating effect also at lower concentrations in co-culture when IL-6 and sIL-6R are constantly produced and secreted. The data nevertheless do not rule out the possibility of other interactive pathways of activation. For example, a reciprocal activation of STAT3 between tumor cells and bone marrow-derived cells has recently been described and shown to be mediated by the sphingosine-1 phosphate receptor 1 (S1PR1), a member of the G protein-coupled receptor family of the lysophospholipids that sustains STAT3 activation by IL-6 (48). Whether S1PR1 plays such a role in sustaining STAT3 activation in neuroblastoma is presently investigated by our laboratories. Our data point to the important role that monocytes could play in EMDR in cancer, a new function recently demonstrated in a mouse model of mammary carcinoma by Denardo *et al.,* who showed that suppression of macrophage infiltration in tumors increases response to chemotherapy (46). A similar protective role of monocytes in cis-platinum-induced apoptosis in colon and lung cancer initiating cells has also been recently reported (47).

Interestingly, our analysis of pSTAT3 expression in bone marrow samples of patients with neuroblastoma revealed the presence of pSTAT3 not only in tumor cells and in $CD45^+$ myeloid cells including $CD68^+$ monocytes/macrophages, but also in a $CD25^+$, $FoxP3^+$ Treg cells. Activation of pSTAT3 in Treg cells has been shown to be mediated by IL-23 produced by TAM under STAT3 activation, which leads to the expression of FoxP3 and the secretion of the immunosuppressive cytokines IL-10 by Treg (49). Finally, we also observed a sub-population of $CD45^-/GD2^-$ bone marrow cells that expressed pSTAT3. Although these cells were not fully characterized at this point, they could represent in part mesenchymal cells that we have shown to play a critical intermediary role in bone invasion in neuroblastoma (13).

Ultimately, our data raise the question whether inhibition of IL-6-mediated STAT3 activation in neuroblastoma could play a role in therapy by preventing EMDR. Several humanized monoclonal antibodies against soluble and membrane bound IL-6R (tocilizumab, REGN88) or against IL-6 (siltuximab and sirukumab) are currently in clinical trials for Castleman's disease, rheumatoid arthritis and several types of cancer (44). Other potentially active agents include small molecule inhibitors of JAK, some of them being currently tested in clinical trials (50, 51). Our data suggest that in neuroblastoma these inhibitors may be most effective in combination with cytotoxic agents to prevent EMDR.

In summary, we provide here a new mechanistic insight on the contributory role of the bone marrow microenvironment in promoting drug resistance in neuroblastoma, as we demonstrate that by being a source of IL-6 and sIL-6R, the bone marrow microenvironment provides tumor cells with the ability to resist the cytotoxic effects of chemotherapy through STAT-3 activation.

Supplementary Material

Refer to Web version on PubMed Central for supplementary material.

Acknowledgments

The authors thank J. Rosenberg for her excellent assistance in preparing the manuscript.

Grant support

The work was supported by an NIH grant PO1 CA 84103 to RCS and YAD, a NIH grant U54 CA163117 to YAD, and a ThinkCure grant to RCS. TA was the recipient of a grant from the Children's Cancer Research Fund and the Children's Neuroblastoma Cancer Foundation.

Reference List

1. Hanahan D, Weinberg RA. Hallmarks of cancer: the next generation. Cell. 2011; 144:646–674. [PubMed: 21376230]
2. Denardo DG, Barreto JB, Andreu P, Vasquez L, Tawfik D, Kolhatkar N, et al. CD4(+) T cells regulate pulmonary metastasis of mammary carcinomas by enhancing protumor properties of macrophages. Cancer Cell. 2009; 16:91–102. [PubMed: 19647220]
3. Tlsty TD, Coussens LM. Tumor stroma and regulation of cancer development. Annu Rev Pathol. 2006; 1:119–150. [PubMed: 18039110]
4. Joyce JA, Pollard JW. Microenvironmental regulation of metastasis. Nat Rev Cancer. 2009; 9:239–252. [PubMed: 19279573]
5. Karnoub AE, Dash AB, Vo AP, Sullivan A, Brooks MW, Bell GW, et al. Mesenchymal stem cells within tumour stroma promote breast cancer metastasis. Nature. 2007; 449:557–563. [PubMed: 17914389]
6. Dalton WS, Hazlehurst L, Shain K, Landowski T, Alsina M. Targeting the bone marrow microenvironment in hematologic malignancies. Semin Hematol. 2004; 41:1–5. [PubMed: 15190509]
7. Meads MB, Gatenby RA, Dalton WS. Environment-mediated drug resistance: a major contributor to minimal residual disease. Nat Rev Cancer. 2009; 9:665–674. [PubMed: 19693095]
8. Shain KH, Yarde DN, Meads MB, Huang M, Jove R, Hazlehurst LA, et al. Beta1 integrin adhesion enhances IL-6-mediated STAT3 signaling in myeloma cells: implications for microenvironment influence on tumor survival and proliferation. Cancer Res. 2009; 69:1009–1015. [PubMed: 19155309]
9. Nefedova Y, Landowski TH, Dalton WS. Bone marrow stromal-derived soluble factors and direct cell contact contribute to de novo drug resistance of myeloma cells by distinct mechanisms. Leukemia. 2003; 17:1175–1182. [PubMed: 12764386]
10. Meads MB, Hazlehurst LA, Dalton WS. The bone marrow microenvironment as a tumor sanctuary and contributor to drug resistance. Clin Cancer Res. 2008; 14:2519–2526. [PubMed: 18451212]
11. Maris JM, Hogarty MD, Bagatell R, Cohn SL. Neuroblastoma. Lancet. 2007; 369:2106–2120. [PubMed: 17586306]
12. Dubois SG, Kalika Y, Lukens JN, Brodeur GM, Seeger RC, Atkinson JB, et al. Metastatic sites in stage IV and IVS neuroblastoma correlate with age, tumor biology, and survival. J Pediatr Hematol Oncol. 1999; 21:181–189. [PubMed: 10363850]
13. Sohara Y, Shimada H, Minkin C, Erdreich-Epstein A, Nolta JA, DeClerck YA. Bone marrow mesenchymal stem cells provide an alternate pathway of osteoclast activation and bone destruction by cancer cells. Cancer Res. 2005; 65:1129–1135. [PubMed: 15734993]
14. Song L, Asgharzadeh S, Salo J, Engell K, Wu HW, Sposto R, et al. Valpha24-invariant NKT cells mediate antitumor activity via killing of tumor-associated macrophages. J Clin Invest. 2009; 119:1524–1536. [PubMed: 19411762]
15. Song L, Ara T, Wu HW, Woo CW, Reynolds CP, Seeger RC, et al. Oncogene MYCN regulates localization of NKT cells to the site of disease in neuroblastoma. J Clin Invest. 2007; 117:2702–2712. [PubMed: 17710228]
16. Ara T, Song L, Shimada H, Keshelava N, Russell HV, Metelitsa LS, et al. Interleukin-6 in the bone marrow microenvironment promotes the growth and survival of neuroblastoma cells. Cancer Res. 2009; 69:329–337. [PubMed: 19118018]
17. Yu H, Pardoll D, Jove R. STATs in cancer inflammation and immunity: a leading role for STAT3. Nat Rev Cancer. 2009; 9:798–809. [PubMed: 19851315]
19. Shuai K, Stark GR, Kerr IM, Darnell JE Jr. A single phosphotyrosine residue of Stat91 required for gene activation by interferon-gamma. Science. 1993; 261:1744–1766. [PubMed: 7690989]
20. Grivennikov S, Karin E, Terzic J, Mucida D, Yu GY, Vallabhapurapu S, et al. IL-6 and Stat3 are required for survival of intestinal epithelial cells and development of colitis-associated cancer. Cancer Cell. 2009; 15:103–113. [PubMed: 19185845]

21. Calo V, Migliavacca M, Bazan V, Macaluso M, Buscemi M, Gebbia N, et al. STAT proteins: from normal control of cellular events to tumorigenesis. J Cell Physiol. 2003; 197:157–168. [PubMed: 14502555]
22. Hirano T, Ishihara K, Hibi M. Roles of STAT3 in mediating the cell growth, differentiation and survival signals relayed through the IL-6 family of cytokine receptors. Oncogene. 2000; 19:2548–2556. [PubMed: 10851053]
23. Aggarwal BB, Kunnumakkara AB, Harikumar KB, Gupta SR, Tharakan ST, Koca C, et al. Signal transducer and activator of transcription-3, inflammation, and cancer: how intimate is the relationship? Ann N Y Acad Sci. 2009; 1171:59–76. [PubMed: 19723038]
24. Bonner JA, Trummell HQ, Willey CD, Plants BA, Raisch KP. Inhibition of STAT-3 results in radiosensitization of human squamous cell carcinoma. Radiother Oncol. 2009; 92:339–344. [PubMed: 19616333]
25. Bewry NN, Nair RR, Emmons MF, Boulware D, Pinilla-Ibarz J, Hazlehurst LA. Stat3 contributes to resistance toward BCR-ABL inhibitors in a bone marrow microenvironment model of drug resistance. Mol Cancer Ther. 2008; 7:3169–3175. [PubMed: 18852120]
26. Ara T, DeClerck YA. Interleukin-6 in bone metastasis and cancer progression. Eur J Cancer. 2010; 46:1223–1231. [PubMed: 20335016]
27. Kishimoto T. Interleukin-6: discovery of a pleiotropic cytokine. Arthritis Res Ther. 2006; 8(Suppl 2):S2. [PubMed: 16899106]
28. Kallen KJ. The role of transsignalling via the agonistic soluble IL-6 receptor in human diseases. Biochim Biophys Acta. 2002; 1592:323–343. [PubMed: 12421676]
29. Schust J, Sperl B, Hollis A, Mayer TU, Berg T. Stattic: a small-molecule inhibitor of STAT3 activation and dimerization. Chem Biol. 2006; 13:1235–1242. [PubMed: 17114005]
30. Nishimoto N. Humanized anti-human IL-6 receptor antibody, tocilizumab. Nippon Rinsho. 2007; 65:1218–1225. [PubMed: 17642235]
31. Keshelava N, Frgala T, Krejsa J, Kalous O, Reynolds CP. DIMSCAN: a microcomputer fluorescence-based cytotoxicity assay for preclinical testing of combination chemotherapy. Methods Mol Med. 2005; 110:139–153. [PubMed: 15901933]
32. Simon T, Langler A, Harnischmacher U, Fruhwald MC, Jorch N, Claviez A, et al. Topotecan, cyclophosphamide, and etoposide (TCE) in the treatment of high-risk neuroblastoma. Results of a phase-II trial. J Cancer Res Clin Oncol. 2007; 133:653–661. [PubMed: 17479288]
33. Molina B, Alonso L, Gonzalez-Vicent M, Andion M, Hernandez C, Lassaletta A, et al. High-dose busulfan and melphalan as conditioning regimen for autologous peripheral blood progenitor cell transplantation in high-risk neuroblastoma patients. Pediatr Hematol Oncol. 2011; 28:115–123. [PubMed: 21299340]
34. Egler RA, Burlingame SM, Nuchtern JG, Russell HV. Interleukin-6 and soluble interleukin-6 receptor levels as markers of disease extent and prognosis in neuroblastoma. Clin Cancer Res. 2008; 14:7028–7034. [PubMed: 18980999]
35. Russell HV, Groshen SG, Ara T, DeClerck YA, Hawkins R, Jackson HA, et al. A phase I study of zoledronic acid and low-dose cyclophosphamide in recurrent/refractory neuroblastoma: A new approaches to neuroblastoma therapy (NANT) study. Pediatr Blood Cancer. 2011; 57:275–282. [PubMed: 21671363]
36. Iwase K, Nagasaka A, Nagatsu I, Kiuchi K, Nagatsu T, Funahashi H, et al. Tyrosine hydroxylase indicates cell differentiation of catecholamine biosynthesis in neuroendocrine tumors. J Endocrinol Invest. 1994; 17:235–239. [PubMed: 7523477]
37. Bowman T, Broome MA, Sinibaldi D, Wharton W, Pledger WJ, Sedivy JM, et al. Stat3-mediated Myc expression is required for Src transformation and PDGF-induced mitogenesis. Proc Natl Acad Sci U S A. 2001; 98:7319–7324. [PubMed: 11404481]
38. Brodeur GM, Seeger RC, Schwab M, Varmus HE, Bishop JM. Amplification of N-myc in untreated human neuroblastomas correlates with advanced disease stage. Science. 1984; 224:1121–1124. [PubMed: 6719137]
39. Gritsko T, Williams A, Turkson J, Kaneko S, Bowman T, Huang M, et al. Persistent activation of stat3 signaling induces survivin gene expression and confers resistance to apoptosis in human breast cancer cells. Clin Cancer Res. 2006; 12:11–19. [PubMed: 16397018]

40. Lassmann S, Schuster I, Walch A, Gobel H, Jutting U, Makowiec F, et al. STAT3 mRNA and protein expression in colorectal cancer: effects on STAT3-inducible targets linked to cell survival and proliferation. J Clin Pathol. 2007; 60:173–179. [PubMed: 17264243]
41. Miller MA, Ohashi K, Zhu X, McGrady P, London WB, Hogarty M, et al. Survivin mRNA levels are associated with biology of disease and patient survival in neuroblastoma: a report from the children's oncology group. J Pediatr Hematol Oncol. 2006; 28:412–417. [PubMed: 16825985]
42. Dalton WS. Drug resistance and drug development in multiple myeloma. Semin Oncol. 2002; 29:21–25. [PubMed: 12520481]
43. Silverman AM, Nakata R, Shimada H, Sposto R, DeClerck YA. A galectin-3-dependent pathway upregulates interleukin-6 in the microenvironment of human neuroblastoma. Cancer Res. 2012; 72:2228–2238. [PubMed: 22389450]
44. Jones SA, Scheller J, Rose-John S. Therapeutic strategies for the clinical blockade of IL-6/gp130 signaling. J Clin Invest. 2011; 121:3375–3383. [PubMed: 21881215]
45. Stasi R, Brunetti M, Parma A, Di Giulio C, Terzoli E, Pagano A. The prognostic value of soluble interleukin-6 receptor in patients with multiple myeloma. Cancer. 1998; 82:1860–1866. [PubMed: 9587117]
46. Denardo DG, Brennan DJ, Rexhepaj E, Ruffell B, Shiao SL, Madden SF, et al. Leukocyte Complexity Predicts Breast Cancer Survival and Functionally Regulates Response to Chemotherapy. Cancer Discov. 2011; 1:54–67. [PubMed: 22039576]
47. Jinushi M, Chiba S, Yoshiyama H, Masutomi K, Kinoshita I, Dosaka-Akita H, et al. Tumor-associated macrophages regulate tumorigenicity and anticancer drug responses of cancer stem/initiating cells. Proc Natl Acad Sci U S A. 2011; 108:12425–12430. [PubMed: 21746895]
48. Lee H, Deng J, Kujawski M, Yang C, Liu Y, Herrmann A, et al. STAT3-induced S1PR1 expression is crucial for persistent STAT3 activation in tumors. Nat Med. 2010; 16:1421–1428. [PubMed: 21102457]
49. Kortylewski M, Xin H, Kujawski M, Lee H, Liu Y, Harris T, Drake C, Pardoll D, Yu H. Regulation of the IL-23 and IL-12 balance by Stat3 signaling in the tumor microenvironment. Cancer Cell. 2009:114–123. [PubMed: 19185846]
50. Jing N, Tweardy DJ. Targeting Stat3 in cancer therapy. Anticancer Drugs. 2005; 16:601–607. [PubMed: 15930886]
51. Verstovsek S. Ruxolitinib: the first agent approved for myelofibrosis. Clin Adv Hematol Oncol. 2012; 10:111–113. [PubMed: 22402352]

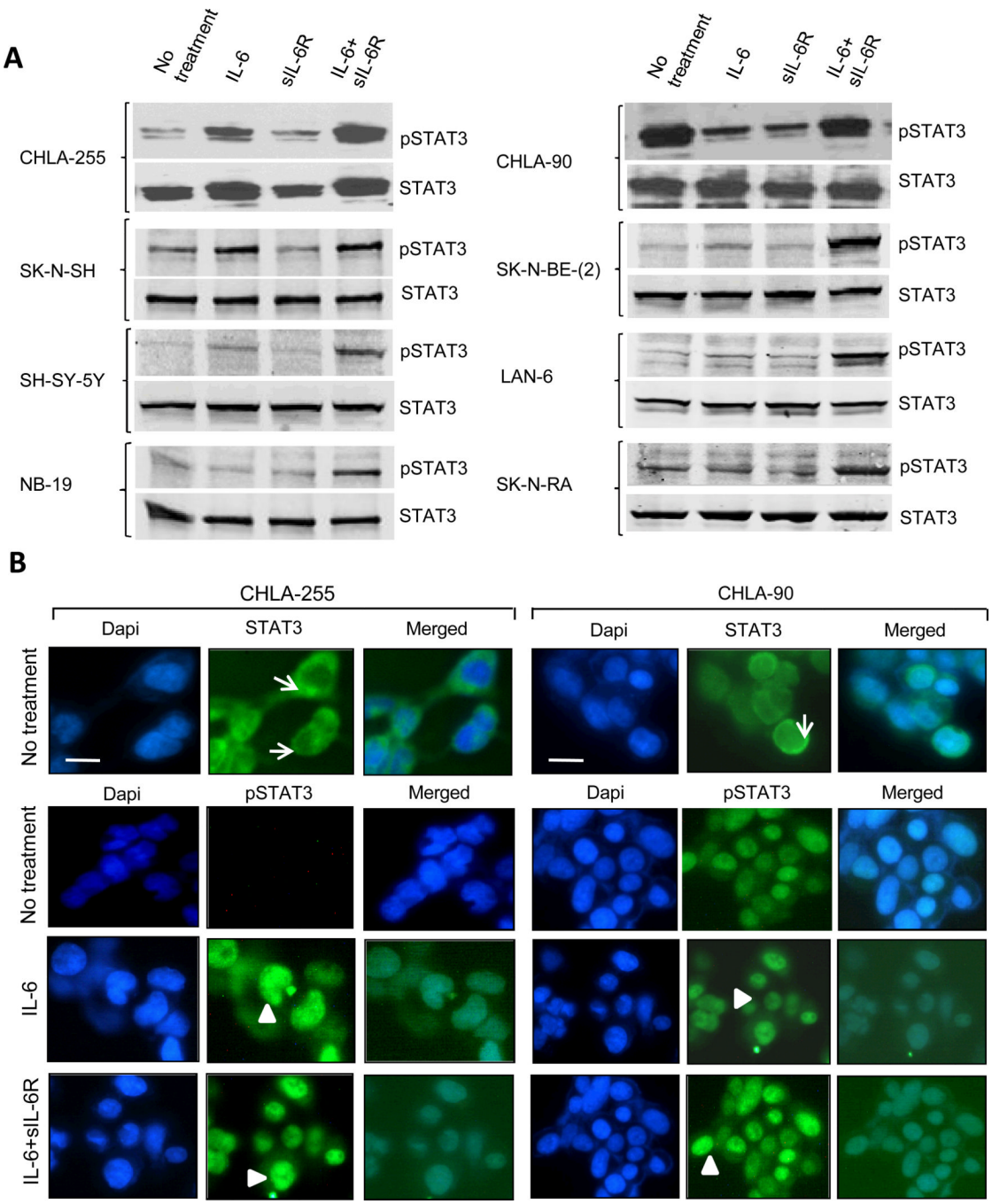

Figure 1.

IL-6 and sIL-6R activate STAT3 in human neuroblastoma cells. A., The presence of phosphorylated pY^{705} STAT3 and STAT3 was detected by Western blot analysis in total cell lysates from 8 neuroblastoma cell lines. When indicated, cells were treated with IL-6 (10 ng/ml), sIL-6R (25 ng/ml). Lysates were obtained 30 minutes after treatment. The data are representative of 2 to 3 separate experiments showing similar results. B, The presence of STAT3 and pY^{705} STAT3 in cultured CHLA-255 (left panel) and CHLA-90 (right panel) cells untreated or treated for 30 minutes with IL-6 alone or with sIL-6R as described above was examined by immunocytofluorescence. Arrow: cytoplasmic STAT3. Arrowhead: nuclear pSTAT3. (Scale bar = 20 μm).

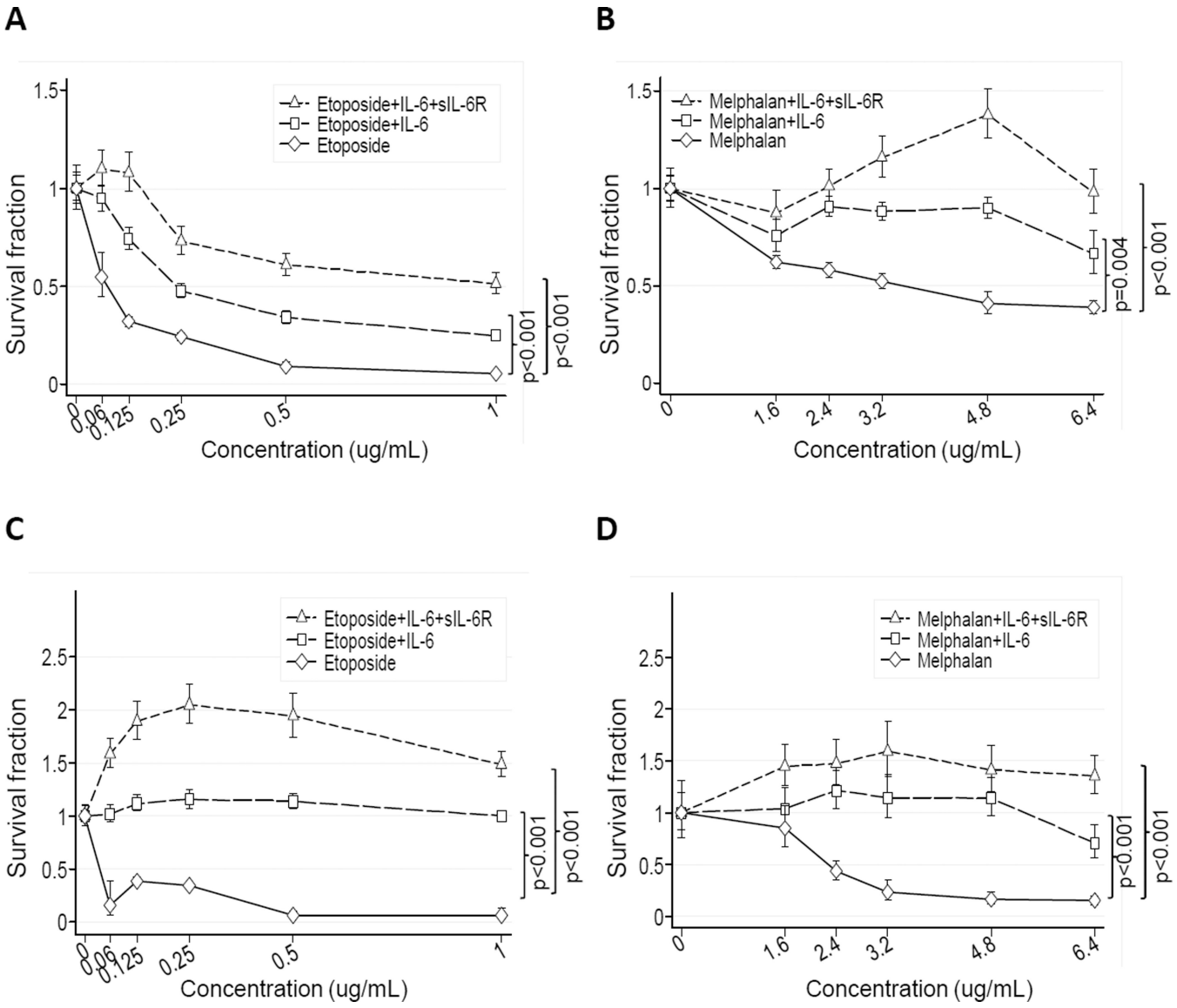

Figure 2.

IL-6 and sIL-6R protect neuroblastoma cells from drug toxicity. CHLA-255 (A and B) and SK-N-SH cells (C and D) were treated with IL-6 (10 ng/mL) alone or with sIL-6R (25 ng/mL) for 24 hours before being exposed to etoposide (A and C) or melphalan (B and D) at indicated concentrations. Cell viability was determined after 24 hours of drug exposure by DIMSCAN analysis. The data represent the mean (±SD) survival fraction with a minimum of 10 replicates for each experimental condition.

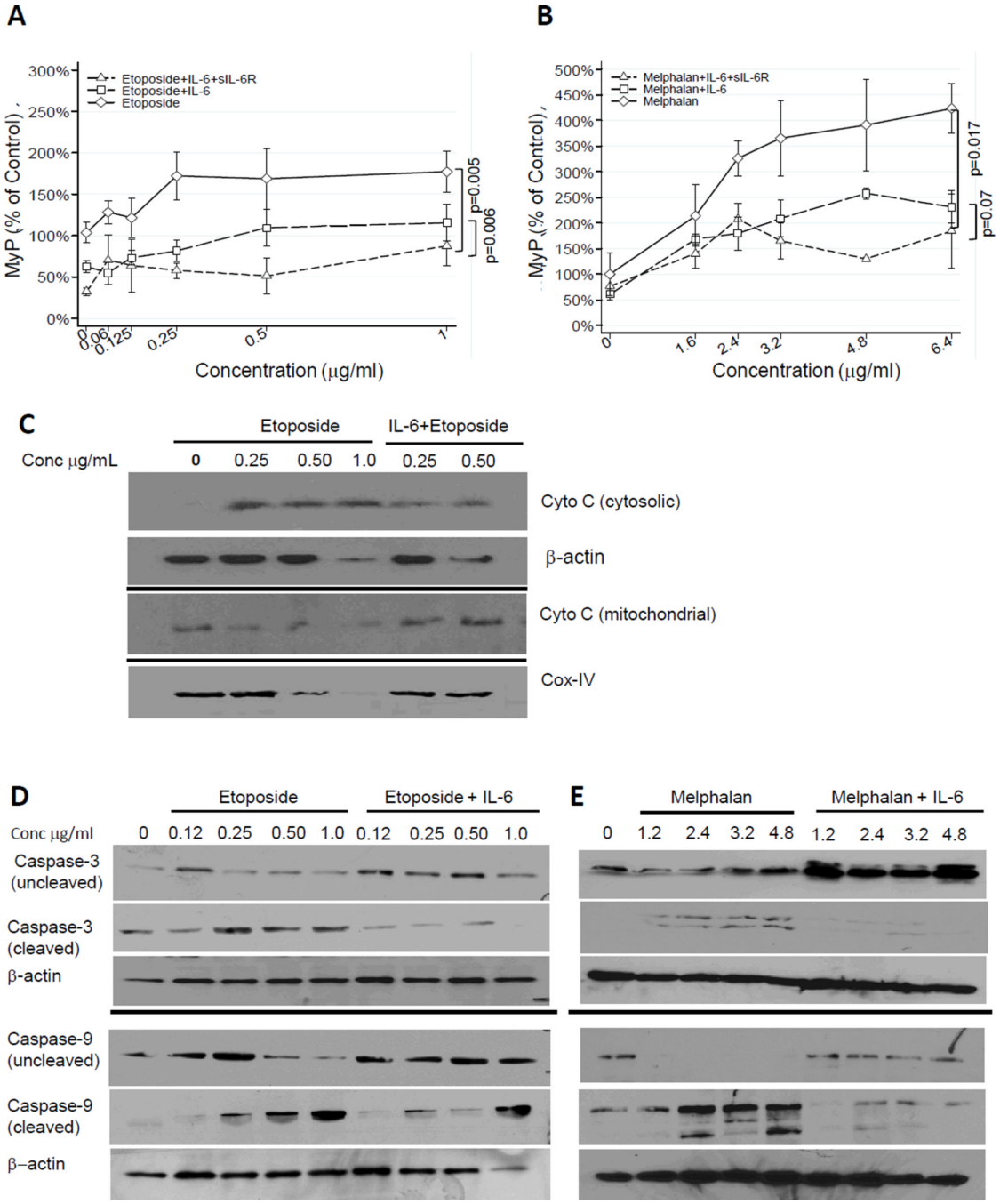

Figure 3.

IL-6 and sIL-6R protect neuroblastoma cells from drug-induced apoptosis. A and B, CHLA-255 cells were treated as in Figure 2. After 24 hours mitochondrial membrane depolarization (MΨP) was examined by JC-1 staining by flow cytometry. The data represent the mean (±SE) percent change in depolarization from control cells (untreated with cytotoxic drugs). C, CHLA-255 cells were treated as above indicated. After 24 hours cytosolic and mitochondrial extracts were examined for the presence of cytochrome C by Western blot. The data are representative of two separate experiments showing similar results. Cox-IV and β-actin were used as loading control for mitochondrial and cytosolic fractions respectively. D and E, CHLA-255 cells were treated with IL-6 and etoposide or

melphalan. After 24 hours of drug exposure, cell lysates were examined for the expression of full length and cleaved caspases 3 and 9. The data are representative of two separate experiments showing similar results. In all gels (C to E), separation lines indicate different gels loaded with the same amount of cell lysate.

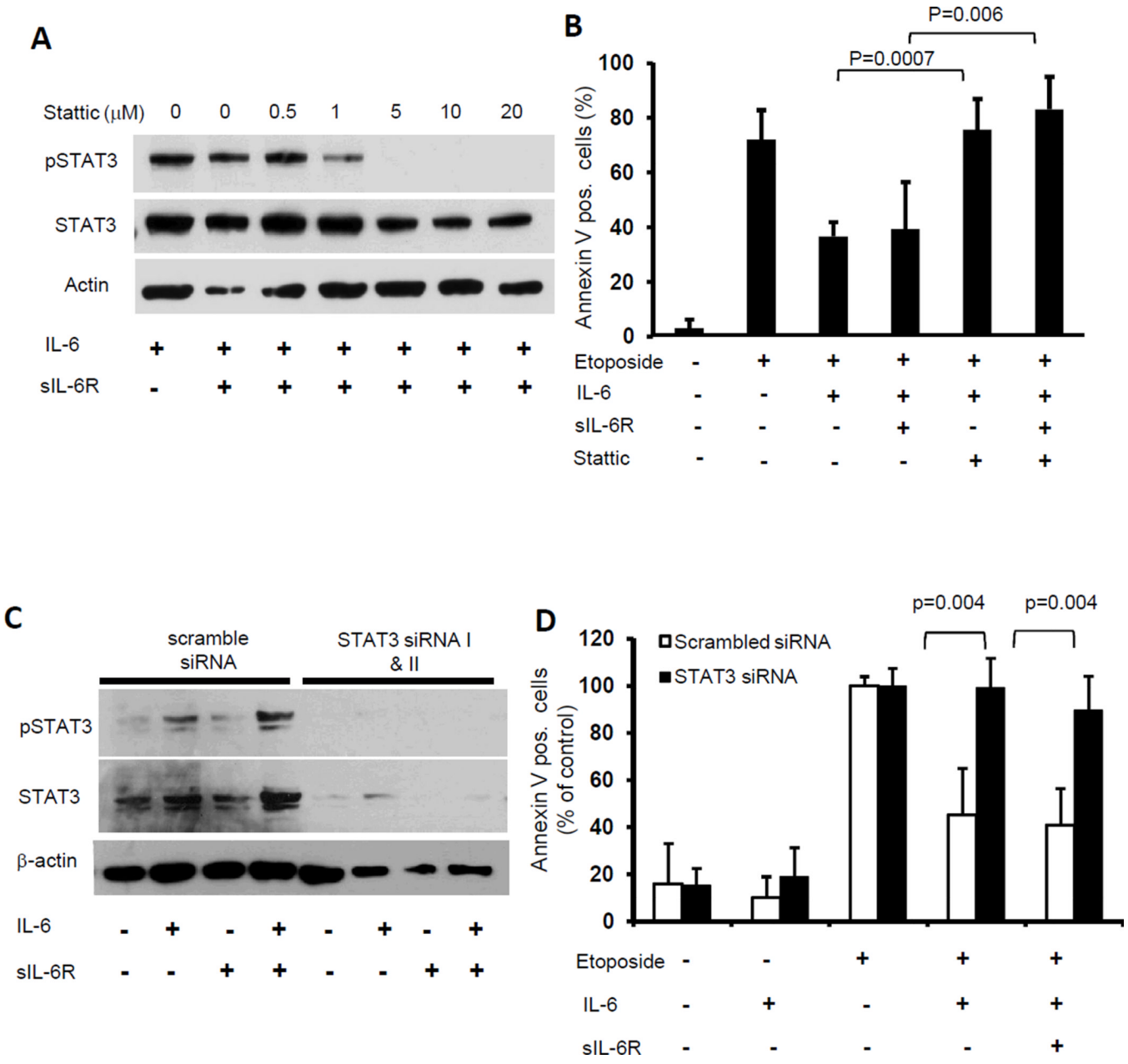

Figure 4.

STAT3 is necessary for IL-6-mediated drug resistance. A, CHLA-255 cells were treated with IL-6 (10 ng/mL) and sIL-6R (25 ng/mL) for 30 minutes in the presence of stattic at indicated concentrations. Cell lysates were examined for pSTAT3 and STAT3 expression by Western blot. B, CHLA-255 cells were treated with stattic (2.5 μM) and IL-6 and sIL-6R for 24 hours before being exposed to etoposide (0.25 μg/mL). After 24 hours cells were examined for Annexin V expression by flow cytometry. The data represent the mean percentage (±SD) of Annexin V positive cells from 4 samples obtained in 3 independent experiments. C, CHLA-255 cells were transfected with STAT3 siRNA or with a scramble sequence. After 72 hours, cells were treated with IL-6 and sIL-6R for 30 minutes and cell lysates were examined for pSTAT3 and STAT3 expression by Western blot. The data are representative of three separate experiments showing similar results. D, siRNA transfected

CHLA-255 cells were treated with IL-6 and sIL-6R for 24 hours before being exposed to etoposide (0.25 μg/mL) and examined for the presence of Annexin V at the cell surface. The data represent the mean percentage (±SD) of Annexin V positive cells compared with control (cells treated with etoposide alone) from 4 samples obtained from 3 independent experiments.

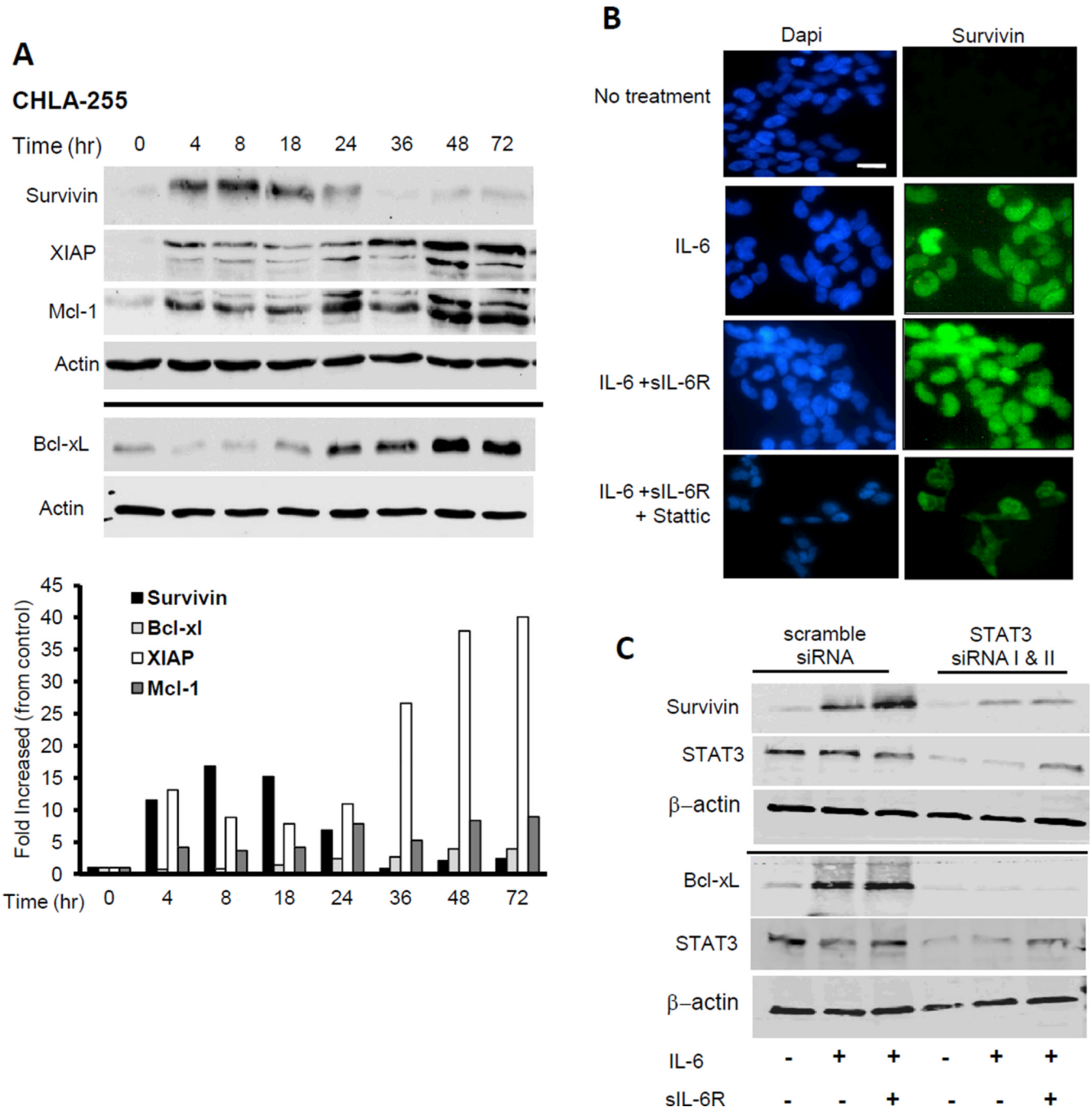

Figure 5.

IL-6 upregulates the expression of anti-apoptotic proteins. A, CHLA-255 cells were treated with IL-6 (10ng/mL) and cells were lysed at indicated time points (hours). Total cell lysates (20μg/lane) were then examined by Western blot for the expression of indicated anti-apoptotic proteins. Actin was used as loading control. The data are representative of 3 separate experiments showing similar results. The bar graph represents the fold increase compared to control after the ratios of anti-apoptotic protein:actin were normalized for the ratio at 0 hour. B, CHLA-255 cells were treated with IL-6 and slL-6R and examined for survivin expression by immunofluorescence. Stattic (2.5 mM) was added 4 hours before IL-6 and sIL-6R when indicated (scale bar = 20μm). C, siRNA transfected CHLA-255 cells

treated as above described were examined for pSTAT3, survivin and Bcl-xL expression by Western blot after 24 hours of stimulation with IL-6 and sIL-6R. The data are representative of 3 experiments showing similar results.

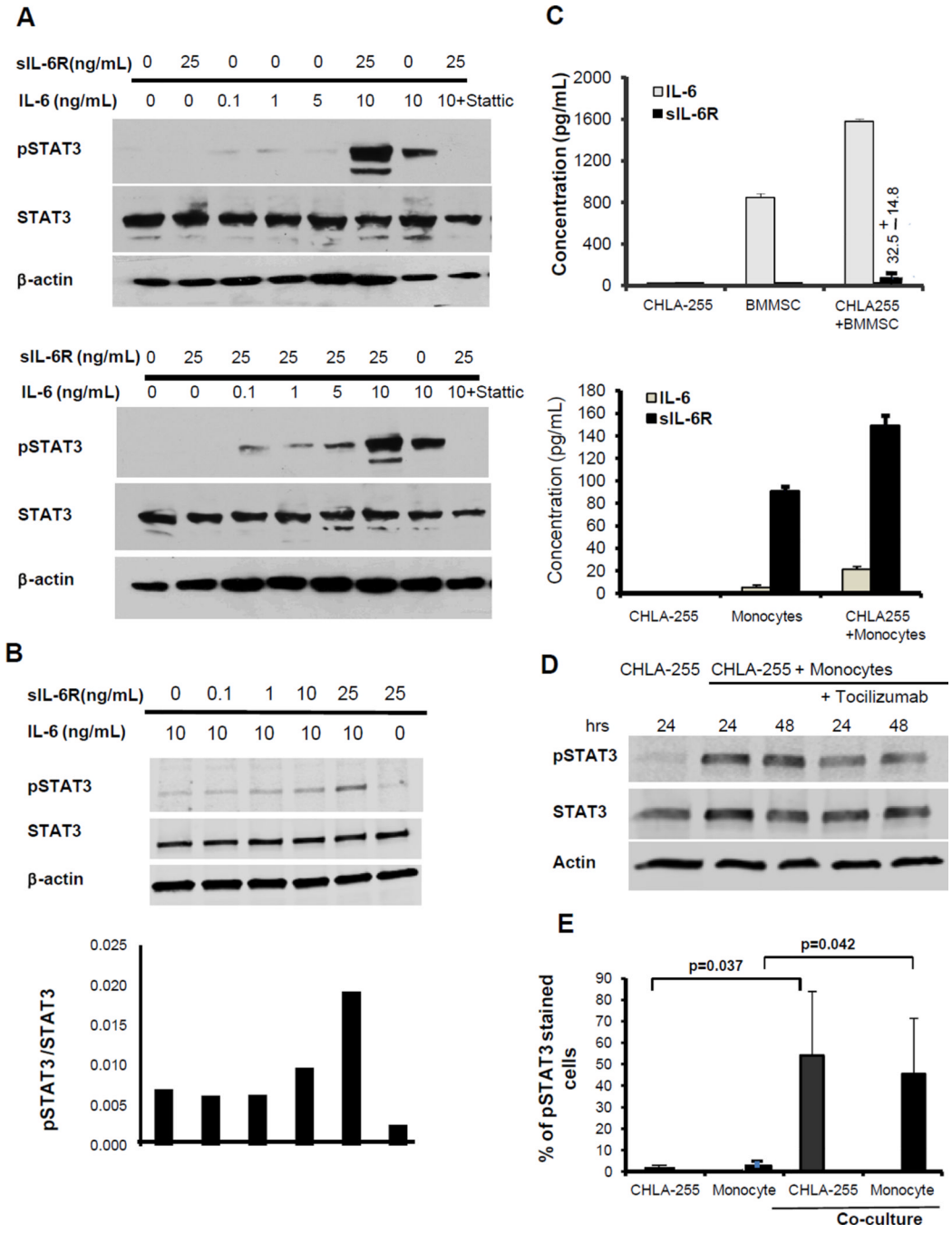

Figure 6.

sIL-6R produced by monocytes sensitizes neuroblastoma cells to IL-6-mediated STAT3 activation. A, CHLA-255 cells were treated with IL-6 at indicated concentrations in the absence (top panel) or presence (lower panel) of sIL-6R (25ng/mL) for 30 minutes. The cell lysates were examined for expression of pSTAT3 and STAT3 by Western blot. B, CHLA-255 cells were treated with IL-6 alone (10 ng/ml) and in the presence of increased concentrations of sIL-6R (0.1 to 25 ng/mL) for 30 minutes. The cell lysates were then examined for expression of pSTAT3 and STAT3 by Western blot. The bar diagram represents the ratio pSTAT3/STAT3 obtained by scanning of the blot. C, CHLA-255 (4.5×10^5) and human BMMSC or monocytes (4.5×10^5) were cultured either alone or

together in Transwell plates for 48 hours. The culture medium was collected and the concentrations of IL-6 and sIL-6R were determined by ELISA. The data represent the mean concentration (±SD) of duplicate (upper) and triplicate (lower) samples. D, CHLA-255 cells were co-cultured with monocytes in Transwell plates in the absence or presence of an anti-IL-6R antibody (tocilizumab). After 48 hours cell lysates were examined for pSTAT3 and STAT3 by Western blot. E. Monocytes isolated from the peripheral blood of patients with neuroblastoma and CHLA-255 cells were cultured alone or in contact (ratio tumor cells:monocytes 4:1) for 24 hours. Cells were then harvested and examined by flow cytometry for the presence of nuclear pSTAT3 and expression of cell surface CD56 and CD14 to separate tumor cells from monocytes. The data represent the average percent of pSTAT3 positive cells (±SD) from 3 separate samples.

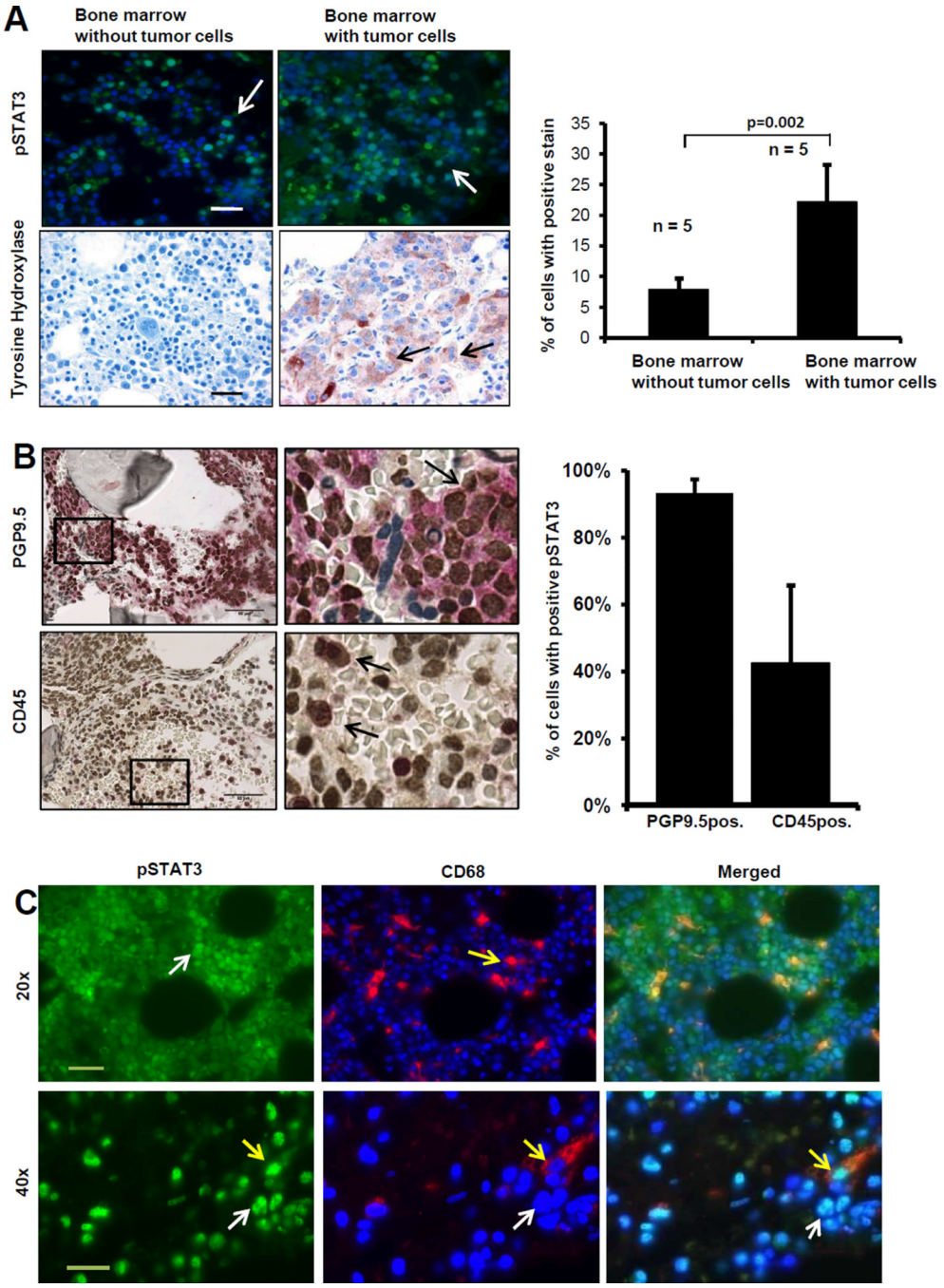

Figure 7.

STAT3 is activated in the bone marrow microenvironment in patients with metastatic neuroblastoma. A, Left panel: Paraffin-embedded sections of bone marrow biopsies from patients (n=10) with neuroblastoma were examined by immunofluorescence for the presence of nuclear pSTAT3 (white arrow) and by immunohistochemistry for the presence of TH positive tumor cells (black arrow) (bar = 50 μm). Right panel: The data represent the mean percentage (±SD) of positive nuclei determined in 5 high magnification (40×) fields per sample (bar = 20μm). B, Bone marrow biopsy infiltrated with > 90% of neuroblastoma cells was examined by dual immunohistochemistry as described in material and methods for the presence of pSTAT3 in PGP9.5^{+} tumor cells (Top) or CD45^{+} myeloid cells (bottom). The

histogram on the right side represents the mean (±SD) percentage of PGP9.5 and CD45 positive cells that were also positive for pSTAT3 from 5 high power field areas (bar = 50 μm). C. The presence of pSTAT3 and CD68 positive cells in bone marrow samples was examined by dual immunofluorescence (white arrows indicate nuclear localization of pSTAT3 in tumor cells and yellow arrows in CD68 positive cells. Bar = 50 μm at 20× and 20 μm at 40×).